

Keratin 6a mutations lead to impaired mitochondrial quality control

S.M. Lehmann, R.E. Leube and N. Schwarz 

Institute of Molecular and Cellular Anatomy, RWTH Aachen University, Aachen, Germany

Linked Comment: Vetter and Magin. *Br J Dermatol* 2020; **182**:529–530.

Summary

Correspondence

Nicole Schwarz.

E-mail: nschwarz@ukaachen.de

Accepted for publication

15 April 2019

Funding sources

Research was funded by IZKF RWTH Aachen University (Start 129/12).

Conflicts of interest

None to declare.

DOI 10.1111/bjd.18014

Background Epidermal differentiation is a multilevel process in which keratinocytes need to lose their organelles, including their mitochondria, by autophagy. Disturbed autophagy leads to thickening of the epidermis as seen in pachyonychia congenita (PC), a rare skin disease caused by mutations in keratins 6, 16 and 17. **Objectives** To ask if mitophagy, the selective degradation of mitochondria by autophagy, is disturbed in PC and, if so, at which stage.

Methods Immortalized keratinocytes derived from patients with PC were used in fluorescence-based and biochemical assays to dissect the different steps of mitophagy. **Results** PC keratinocytes accumulated old mitochondria and displayed disturbed clearance of mitochondria after mitochondrial uncoupling. However, early mitophagy steps and autophagosome formation were not affected. We observed that autolysosomes accumulate in PC and are not sufficiently recycled.

Conclusions We propose an influence of keratins on autolysosomal degradation and recycling.

What's already known about this topic?

- Terminal epidermal differentiation is a multistep process that includes the elimination of cellular components by autophagy.
- Autophagy-impaired keratinocytes have been shown to result in thickening of epidermal layers.
- Hyperkeratosis also occurs in pachyonychia congenita (PC), a rare skin disease caused by mutations in keratins 6, 16 and 17.

What does this study add?

- Keratins contribute to mitochondrial quality control as well as maintenance of mitochondria–endoplasmic reticulum contact sites.
- Keratins influence autolysosomal maturation or reformation.

What is the translational message?

- Overaged mitochondria and autolysosomes accumulate in PC.
- Mutations in keratin 6a lead to severely impaired mitophagy, which might contribute to PC pathogenesis.

Keratin intermediate filaments are present in all epithelial cells, where they are critical for stress protection and maintenance of cellular integrity. Equal amounts of type I and type II keratins assemble into cytoplasmic networks that are anchored to desmosomes and hemidesmosomes. Mutations in keratin genes

result in more than 30 human diseases, including the rare skin disease pachyonychia congenita (PC).¹

PC is caused by mutations in type II keratins 6a, 6b and 6c, and type I keratins 16 and 17. PC is characterized by palmoplantar keratoderma and hypertrophic nail dystrophy.^{2,3}

Keratin 6, 16 and 17 expression is upregulated when stratified epithelia encounter stressful situations such as wounding and ultraviolet light exposure.⁴

Recently, intermediate filaments were shown to influence mitochondrial structure, localization and function.⁵ Keeping the cellular mitochondrial pool as healthy as possible is crucial for overall mitochondrial function; therefore mitochondrial turnover is an essential part of mitochondrial quality control.⁶ This is accomplished either by selective elimination of dysfunctional mitochondria through selective macroautophagy (mitophagy) or by renewal of the mitochondrial network through constant fusion and fission of existing mitochondria. Disturbed mitochondrial quality control results in the accumulation of damaged mitochondria, which produce less ATP and release high levels of reactive oxygen species (ROS). One of the best studied mitophagy pathways relies on PINK1 (serine/threonine-protein kinase PINK1, mitochondrial, also known as PTEN-induced putative kinase 1) and Parkin (E3 ubiquitin-protein ligase parkin).⁶ PINK1 is targeted to and usually imported into mitochondria, where it is cleaved by PARL (presenilins-associated rhomboid-like protein, mitochondrial) and then degraded.⁷ Depolarization of the outer mitochondrial membrane (OMM) results in the stabilization of PINK1 on the OMM and subsequent recruitment of Parkin, which attaches ubiquitin moieties to OMM proteins.⁸ This, in turn, recruits ubiquitin- and LC3- (microtubule-associated proteins 1A/1B light-chain 3) binding autophagic adaptor proteins such as p62/SQSTM1 (ubiquitin-binding protein p62, also known as sequestosome-1) or optineurin, in order to induce autophagosome formation around damaged mitochondria.^{9–11} Autophagosomes are transported to and fuse with lysosomes to form autolysosomes. This fusion is required for acidification and degradation of the autophagosome's cargo. In mammalian cells, fusion of autophagosomes and lysosomes is controlled by Rab proteins, which belong to the Ras-like GTPase superfamily. One of its members, Rab7, has been implicated in the maturation of autolysosomes.¹² Rab7 has been shown to directly interact with vimentin, an intermediate filament protein, modulating vimentin's phosphorylation state and therefore its solubility.¹³ Furthermore, disruption of the keratin filament network by treatment of cells with the phosphatase inhibitor okadaic acid inhibits autophagy.¹⁴ In order to restore lysosomes, autolysosomes are recycled through a process called autophagic lysosome reformation in which tubules extrude from autolysosomes and form protolysosomes that mature into lysosomes.¹⁵

Epidermal differentiation strongly depends on macroautophagy.^{16,17} While autophagy per se sustains cell health it is also needed for organelle removal during keratinocyte differentiation. This is accomplished by multiple processes including mitophagy. As PC is characterized by an epidermal hyperproliferation phenotype in conjunction with delayed terminal differentiation, we asked whether PC-linked keratin 6a (K6a) mutations contribute to a mitophagy defect. Indeed, we could show that mitophagy is impaired due to disturbed autolysosomal reformation.

Materials and methods

Cells

The wild-type human keratinocyte cell line (K6a wt) was obtained by immortalization of normal human epidermal keratinocytes using the human papillomavirus (HPV) E6/E7 method and was kindly provided by Drs Julia Reichelt, Verena Wally and Thomas Lettner (EB Haus Austria, Salzburg, Austria). The PC cell lines K6aN171K and K6aN171del were derived from patients, similarly by immortalization of epidermal keratinocytes with the HPV E6/E7 method (generously provided by Dr Leonard M. Milstone, Yale Dermatology Associates, New Haven, CT, U.S.A.).¹⁸

All cell lines were cultured in EpiLife Medium (Thermo Fisher Scientific, Waltham, MA, U.S.A.) supplemented with 10% (v/v) antibiotic-antimycotic solution comprising penicillin, streptomycin and amphotericin B (fungizone; Sigma-Aldrich, St Louis, MO, U.S.A.), and 10% (v/v) human keratinocyte growth factor, in a 5% CO₂ humidified atmosphere at 37 °C. Cell lines were cultured in uncoated cell culture flasks or on glass coverslips coated with rat tail collagen I (Corning, Corning, NY, U.S.A.). The cell lines were passaged once or twice per week at a ratio of 1 : 3. For passaging, cells were washed and incubated for 15 min in phosphate-buffered saline (PBS) without Ca²⁺/Mg²⁺ and thereafter incubated for ~10 min with Accutase (Thermo Fisher Scientific) and resuspended in Trypsin Neutralizer Solution (Thermo Fisher Scientific). Cells were used within 10 passages. Passages were equal for PC cell lines and 10 times higher for wt control. For experiments under differentiation conditions, cells were switched from standard culture, low calcium medium (0.06 mmol L⁻¹ Ca²⁺) to high calcium medium (1.2 mmol L⁻¹ Ca²⁺) for 3 days.

Antibodies

Primary polyclonal rabbit antibody against PINK1 (1 : 1000 for immunoblot; ab23707) was obtained from Abcam (Cambridge, U.K.), antibodies against PTEN (1 : 1000 for immunoblot; 9559) and PI3K (1 : 1000 for immunoblot; 4292) were from Cell Signaling Technology (Danvers, MA, U.S.A.) and antibody against beta-actin (1 : 2000 for immunoblot; A2066) was from Sigma-Aldrich. Monoclonal rabbit antibody against optineurin (1 : 1000 for immunoblot; mAb #58981) was obtained from Cell Signaling Technology. Polyclonal guinea pig antibody against p62/SQSTM1 C-terminus (1 : 1000 for immunoblot; GP62-C) was purchased from Progen Biotechnik (Heidelberg, Germany). Secondary horseradish peroxidase (HRP)-coupled antibodies against rabbit (1 : 5000 for immunoblot; P0448) and against guinea pig (1 : 5000 for immunoblot; P0141) were obtained from Agilent Dako (Santa Clara, CA, U.S.A.).

Immunoblot analysis

Cells were prepared by first washing them with PBS in the culture dish, then 100 µL of 2× sodium dodecyl sulfate (SDS) buffer [100 mmol L⁻¹ Tris-HCl (pH 8), 10% (v/v) glycerol,

3% (w/v) SDS, 7.5% (v/v) β -mercaptoethanol, 250 $\mu\text{g mL}^{-1}$ bromophenol blue] was added and the lysed cells scraped off with a rubber policeman. Cell lysates were stored at $-20\text{ }^{\circ}\text{C}$. Proteins were denatured at $95\text{ }^{\circ}\text{C}$ for 5 min and subsequently separated by 8–14% discontinuous SDS-polyacrylamide gel electrophoresis. Protein transfer onto polyvinylidene difluoride (PVDF) membrane was performed in the presence of transfer buffer (25 mmol L^{-1} Tris-HCl, 190 mmol L^{-1} glycine, 20% methanol) at 100 V for 1 h. The PVDF membrane was blocked with 10% Roti-Block blocking reagent (Carl Roth, Karlsruhe, Germany) for 1 h. After incubation with the primary antibody diluted in 10% Roti-Block overnight at $4\text{ }^{\circ}\text{C}$, the membrane was washed three times for 10 min with TBS-T [130 mmol L^{-1} NaCl, 50 mmol L^{-1} Tris base, 0.1% (v/v) Tween 20]. The membrane was incubated with the secondary HRP-conjugated antibody diluted in 10% Roti-Block for 1 h. After repeated washing with TBS-T, visualization of bound antibodies was done with the help of an enhanced chemiluminescence method and detection using the Fusion Solo (Vilber, Marne-la-Vallée, France). Densitometric evaluation was performed using ImageJ Fiji (National Institutes of Health, Bethesda, MD, U.S.A.).^{19,20} To perform incubation of further antibodies on the same membrane, the membrane was incubated in stripping buffer (0.1 mol L^{-1} glycine, pH 2) 3 \times for 20 min to remove the bound antibodies. Subsequent procedures started with a blocking step and continued as described. Three independent experiments were performed.

Quantitative polymerase chain reaction

RNA was isolated using the RNeasy Mini Kit (Qiagen, Hilden, Germany) according to the manufacturer's protocol. RNA concentration and quality was determined using a NanoDrop 1000 (Thermo Fisher Scientific). Ratios of absorbance at 260 nm and 280 nm were between 1.74 and 2.1. Reverse transcription into cDNA was performed using Transcriptor First Strand cDNA Synthesis Kit (Roche Molecular Systems, Inc., Pleasanton, CA, U.S.A.) according to the manufacturer's protocol. Quantitative real time polymerase chain reaction (qPCR) was performed using the FastStart Essential DNA Probes Master kit (Roche) according to the manufacturer's protocol on a LightCycler 96 Real-Time PCR System (Roche). The cDNA was diluted 1 : 5 in H_2O , a standard was prepared by pooling cDNA of every sample, and a dilution series was generated (1 : 2, 1 : 4, 1 : 8, 1 : 16, 1 : 32).

The following primers were used: HPRT (UPL probe #22) forward (5'-TGATAGATCCATTCTATGACTGTAGA-3') and reverse (5'-CAAGACATTCTTCCAGTTAAAGTTG-3'); PINK1 (UPL probe #65) forward (5'-GCCATCAAGATGATGTGGAAC-3') and reverse (5'-GACCAGCTCCTGGCTCATT-3'); PARL (UPL probe #17) forward (5'-GCTCACTGCGGTCCTAAC-3') and reverse (5'-CTGAATCCGCATTTTGTG-3'); PARK2 (Parkin) (UPL probe #85) forward (5'-GGAGCTGAGGAATGACTGGA-3') and reverse (5'-ACAATGTGAACAATGCTCTGCT-3'); p62/SQSTM1 (UPL probe #14) forward (5'-AGCTGCCTGTACC-CACATC-3') and reverse (5'-CAGAGAAGCCCATGGACAG-3');

optineurin (UPL probe #72) forward (5'-AACAGTGACCCT-GAGCGAAG-3') and reverse (5'-AAGTTGGGTTTACA-GAGGCGTA-3'); and HDAC6 (UPL probe #58) forward (5'-AGTTCACCTTCGACCAGGAC-3') and reverse (5'-GCCAGAACC-TACCCTGCTC-3'). RNA from three independent experiments was analysed in duplicates for each condition.

For quantification, efficiency and CT values were determined using LightCycler 96 software (Roche). Fold factor was calculated as $E_{\text{goi}}^{(\Delta\text{CT}_{\text{goi}})}/E_{\text{ref}}^{(\Delta\text{CT}_{\text{ref}})}$, where goi = gene of interest and ref = reference gene).

MitoTimer

Cells were seeded on day 0 on glass-bottom dishes (14-mm diameter, thickness no. 1.5; MatTek, Ashland, MA, U.S.A.) coated with rat tail collagen I (Corning). After 2 days, cells were transfected with the pMitoTimer Addgene plasmid #52659 (gift from Zhen Yan; <http://n2t.net/addgene:52659>) and were imaged 3 or 4 days after seeding. Live cell imaging was done on a Zeiss LSM 710 DUO microscope (Carl Zeiss Microscopy, Jena, Germany) at $37\text{ }^{\circ}\text{C}$. The 488-nm line of an argon/krypton laser was used for fluorescence recording via a $63\times$ magnification/1.4 numerical aperture/differential interference contrast M27 ($63\times/1.40$ N.A. DIC M27) oil immersion objective (Carl Zeiss). The emitted light was monitored in the range 500–540 nm (green signal) and 580–640 nm (red signal) with a pinhole set at 1–2 Airy units and a laser intensity of 0.2%. Using ImageJ Fiji, green and red channels were thresholded (using Otsu's algorithm) and a mask of regions of interest was calculated that shows the signal as positive in either channel. Fluorescence intensity mean values were determined for every region of interest. Three independent experiments were performed with 30 cells each per condition. Data were normalized to untreated K6a wt cells.

Induction of mitophagy

Cells were seeded on collagen-coated coverslips on day 0 and transfected with a green fluorescent protein–Parkin (eGFP–Parkin) plasmid construct (provided by Sven Geisler, Tübingen, Germany) on day 1 using Xfect (Takara Bio Inc., Shiga, Japan), according to the manufacturer's protocol. On day 2 the cells were treated with $10\text{ }\mu\text{mol L}^{-1}$ carbonyl cyanide *m*-chlorophenyl hydrazone (CCCP) at $37\text{ }^{\circ}\text{C}$ for 2 h and 18 h or with dimethyl sulfoxide only for 18 h as a control. After 2×15 min washing with medium at $37\text{ }^{\circ}\text{C}$, cells were stained with 100 nmol L^{-1} MitoTracker Red CMXRos (Thermo Fisher Scientific) for 30 min at $37\text{ }^{\circ}\text{C}$. After fixation with 4% warm paraformaldehyde (PFA) in diethylpyrocarbonate (DEPC) water for 25 min at room temperature (RT), nuclei were stained with Hoechst 33342 (Thermo Fisher Scientific) and the coverslips were mounted with Mowiol (Carl Roth). Using the Apotome.2 microscope (Carl Zeiss), cells were imaged using the $63\times/1.40$ N.A. DIC M27 oil immersion objective. Imaging of one experiment was performed on the same day for all conditions, with equal exposure times for interference contrast, MitoTracker and

eGFP-Parkin. Using ImageJ Fiji, the mitochondrial area per cell was determined for Parkin-positive cells after background subtraction (rolling ball set to 5). Parkin distribution was scored as cytoplasmic or dotted. Three independent experiments were performed with ≥ 48 cells per condition.

LC3

Cells were seeded at day 0 on collagen-coated coverslips. They were transfected on day 3 with the pftLC3 Addgene plasmid #21074 (gift from Tamotsu Yoshimori, <http://n2t.net/addgene:21074>).²¹ On day 4 the low calcium medium ($0.06 \text{ mmol L}^{-1} \text{ Ca}^{2+}$) was replaced with high calcium medium ($1.2 \text{ mmol L}^{-1} \text{ Ca}^{2+}$) and cells were further propagated for 3 days prior to fixation with 4% PFA in DEPC water for 25 min at RT. Nuclei were stained with Hoechst 33342 and the coverslips were mounted with Mowiol. Using the Apotome.2 microscope, ≥ 16 transfected cells per treatment were imaged with the $63\times/1.40 \text{ N.A. DIC M27}$ oil immersion objective with equal exposure times for interference contrast, green and red channels. Using ImageJ Fiji, LC3-positive puncta were automatically determined in the green and red channels with the help of the 'analyse particles' function (size 5–50 pixels) after background subtraction (rolling ball set to 20). Particles positive in only one channel were scored as either green or red, and particles positive in both channels were scored as yellow. Three independent experiments were performed with ≥ 16 cells per condition.

Electron microscopy

Pelleted cells were fixed in 4% formaldehyde/1% glutaraldehyde for 2 h and in 1% OsO_4 for 1 h. Fixed samples were treated with 0.5% uranyl acetate in 0.05 mol L^{-1} sodium maleate buffer (pH 5.2) for 2 h in the dark, and thereafter dehydrated and embedded in Araldite using acetone as the intermedium. Polymerization was performed at 60°C for 48 h. Semi- and ultrathin sections were prepared with a Leica Ultramicrotome (Leica Microsystems, Wetzlar, Germany) using a diamond knife. To enhance contrast, sections were treated with 3% uranyl acetate for 5 min and with 0.08 mol L^{-1} lead citrate solution for 3 min. Images were taken on a Zeiss EM-10 transmission electron microscope (Carl Zeiss) with a digital camera (Olympus Corporation, Shinjuku, Japan) using iTEM software (Olympus). Analyses were done on $\times 50000$ magnification images. Using ImageJ Fiji, ≥ 50 mitochondria per cell line were encircled to calculate their circumference. Close endoplasmic reticulum (ER) membranes were defined as no more than 15 pixels away from the mitochondrial membrane and their length was determined to calculate the ratio of ER-covered mitochondrial circumference vs. whole mitochondrial circumference.

Statistical analysis

Each experiment was performed at least three times. The numbers of analysed cells are indicated for each

experiment. Differences between groups were evaluated using GraphPad Prism 5.0 (GraphPad Software, La Jolla, CA, U.S.A.) using one-way ANOVA with either Dunnett's or Bonferroni post-hoc tests. Data are summarized and presented as mean \pm SD. Differences were considered significant when $P \leq 0.05$.

Results

Old mitochondria accumulate in pachyonychia congenita keratinocytes

To investigate PC pathology, immortalized keratinocytes were prepared from patients and healthy individuals by viral E6/E7 transformation. For the current study, two PC-derived cell lines producing either K6aN171K or K6aN171del mutants were examined together with a cell line prepared from a healthy donor producing only K6a wt. To find out whether mitochondrial quality control is compromised in PC keratinocytes, cells were transfected with MitoTimer. MitoTimer is a mitochondria-targeting dsRed derivative whose fluorescence shifts from green to red over time as the protein ages.²² Ageing of MitoTimer takes approximately 48 h after initiation of expression. Differences in red/green fluorescence intensity ratios between wt control and patient-derived cells could not be observed 24 h after transfection. However, fluorescence microscopy revealed a significant shift towards red of MitoTimer 2 days after transfection in both types of patient-derived cells but not in wt control cells (Fig. 1). We therefore conclude that mitochondria become older in PC cells than in wt control cells.

Mitochondria–endoplasmic reticulum contact sites are reduced in pachyonychia congenita

Next, electron microscopy was performed to examine mitochondrial ultrastructure. No obvious differences in mitochondrial morphology could be identified at first glance (Fig. 2b–d). However, more careful analysis revealed striking differences in ER–mitochondrial arrangement. While 23% of the circumference of mitochondria in control cells was covered by ER, only 9.8% and 8%, respectively, were covered in the patient cell lines K6aN171K and K6aN171del (Fig. 2a).

Mitochondria–ER contact sites are known as mitochondria-associated membranes (MAMs) and are implicated in mitochondrial quality control. Loss of MAMs leads to reduced mitophagy resulting in accumulation of old and dysfunctional mitochondria.²³

Expression of early mitophagy-related proteins is not altered in pachyonychia congenita keratinocytes

Mitophagy comprises a series of events starting with the accumulation of PINK1 on dysfunctional mitochondria and subsequent recruitment of Parkin. Under normal conditions, PINK1

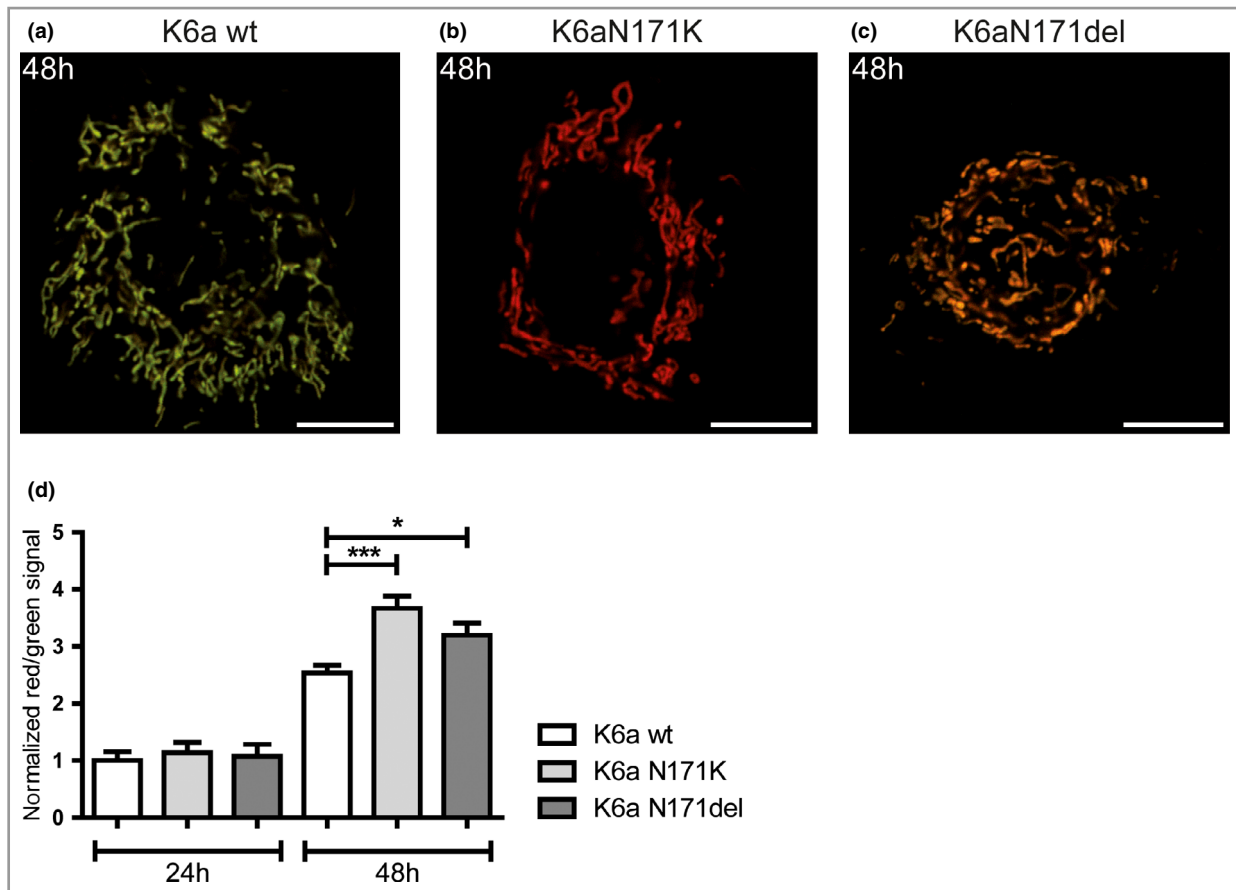


Fig 1. Old mitochondria accumulate in pachyonychia congenita keratinocytes. Cells were transfected with MitoTimer encoding a mitochondrial-targeted dsRed derivative whose fluorescence shifts from green to red with increasing time after synthesis. Fluorescence images were recorded 24 h and 48 h after transfection. (a–c) Representative fluorescence micrographs taken from keratin 6a (K6a) wild-type (wt) and mutant, K6aN171K and K6aN171del keratinocytes 48 h after transfection. Each micrograph depicts an overlay of the green and red channel. Scale bars = 10 μm . (d) The histogram shows the ratiometric quantification of three independent experiments of 30 cells per cell line each. Ratios were normalized to control K6a wt cells 24 h after transfection. MitoTimer changes its colour from green to red over the course of 48 h. No differences in red/green ratios could be observed 24 h after transfection. In contrast, after 48 h, K6aN171K and K6aN171del keratinocytes displayed a significantly increased red/green ratio of fluorescence intensity compared with K6a wt cells. Comparisons with 24-h post-transfection K6a wt cells were performed using one-way ANOVA with Dunnett's post-hoc test. * $P < 0.05$, *** $p < 0.001$.

is imported into mitochondria and cleaved by mitochondrial PARL. On mitochondrial dysfunction, PINK1 accumulates on mitochondria due to its autophosphorylation on two known phosphorylation sites.²⁴

Cells were grown either in low calcium medium (0.06 $\text{mmol L}^{-1} \text{Ca}^{2+}$) or high calcium medium (1.2 $\text{mmol L}^{-1} \text{Ca}^{2+}$) for 3 days to induce differentiation. During differentiation, keratinocytes undergo a series of changes including the loss of their mitochondria by mitophagy. qPCR analysis revealed no significant changes in PINK1, PARL and Parkin mRNA expression in either low- or high calcium medium (Fig. 3a–c). Similarly, PINK1 protein expression was unaltered (Fig. 3d), while PTEN and its counterpart PI3K were reduced in PC cells independently of calcium addition (Fig. 3e, f), although their ratios were unaltered. These results suggest that recognition and marking of dysfunctional mitochondria for subsequent mitophagy are not disturbed.

Mitophagy is impaired in pachyonychia congenita keratinocytes

Although PINK1 is present in both PC cell lines, old mitochondria still accumulate and are not disposed of. We therefore asked if Parkin is recruited to mitochondria following PINK1 stabilization on the outer mitochondrial membrane. To this end, healthy control and PC cells were transfected with fluorescent Parkin to visualize its translocation. Mitophagy was induced by adding the mitochondrial uncoupler CCCP. CCCP treatment led to the translocation of Parkin to mitochondria within 2 h (Fig. 4a). Mitochondria were eliminated by mitophagy after 18 h (Fig. 4a) in control cells. Untreated cells showed an even cytoplasmic distribution of eGFP-Parkin (100% of control cells, 99% of K6aN171K PC cells and 100% of K6aN171del PC cells) (Fig. 4a–c upper panels; quantification in Fig. 4d). Two hours after mitophagy induction by

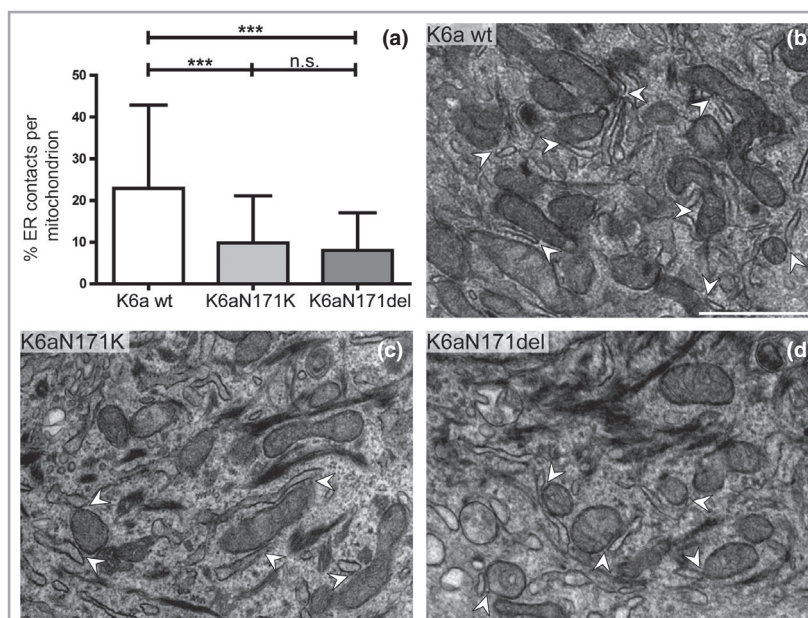


Fig 2. Mitochondrial–endoplasmic reticulum (ER) contact is reduced in pachyonychia congenita keratinocytes. Electron microscopy was performed to investigate the spatial relationship between mitochondria and ER. (a) Histogram of the quantitative analysis of ER contact with mitochondria in the keratin 6a (K6a) mutants K6aN171K, K6aN171del and control cells ($n \geq 50$ mitochondria per cell line). (b–d) Selected electron micrographs depicting examples of mitochondria–ER contact sites in K6a wild-type (wt) (b); K6aN171K (c); and K6aN171del (d) keratinocytes (indicated by arrowheads). Note the significant reduction of contact sites in the mutant cells. Scale bars = 100 nm. Comparisons between groups were performed using one-way ANOVA with Bonferroni post-hoc test. *** $p < 0.001$; n.s., not significant.

CCCP, 93% of control cells, 95% of K6aN171K PC cells and 95% of K6aN171del PC cells showed a dotted eGFP–Parkin pattern colocalizing with MitoTracker staining (Fig. 4a–c middle panels; quantification in Fig. 4d). Hence, Parkin recruitment to dysfunctional mitochondria is not affected by K6a mutations. Eighteen hours after mitophagy induction by CCCP, 73% of control cells showed a restored steady-state cytoplasmic Parkin pattern and lost their mitochondria. In contrast, only 9% of K6aN171K PC cells and 10% of K6aN171del PC cells displayed a cytoplasmic Parkin pattern again and lost their mitochondria, while the remaining fraction of cells still had Parkin recruited to their mitochondria (Fig. 4a–c lower panels; quantification in Fig. 4d). Accordingly, the percentage of the area of mitochondrial signal per cell was not reduced in K6aN171del, while K6aN171K and K6 wt controls showed a reduced mitochondrial signal (Fig. 4e). Of note, in K6aN171K cells the mitochondrial signal decline only occurred within the first 2 h of CCCP treatment whereas in K6a wt a reduction could be observed between all time points. This leads to the conclusion that while dysfunctional mitochondria are marked for mitophagy and Parkin is recruited to mitochondria, subsequent steps of mitophagy are disturbed in PC.

Markers for autophagosome formation are not altered in pachyonychia congenita keratinocytes

To further narrow down which step of mitophagy is impaired in PC, we investigated the expression of mitophagy and

autophagosome markers. After translocation of Parkin, OMM proteins become highly ubiquitinated, which is recognized by the ubiquitin-binding histone deacetylase (HDAC)6 and the autophagy receptors p62/SQSTM1 and optineurin. p62/SQSTM1 mediates the aggregation of dysfunctional mitochondria and directly binds to the autophagic effector proteins LC3A and LC3B.^{9,10} Optineurin becomes recruited to damaged mitochondria, marking the site of initial autophagosome formation.¹¹ HDAC6 promotes autophagy by mediating the attachment of autophagosomes to dynein motors for transport to lysosomes.²⁵ Furthermore, HDAC6 induces cortactin-dependent actin remodelling to facilitate autophagosome–lysosome fusion.²⁶

Optineurin, HDAC6 and p62/SQSTM1 mRNA expression was unchanged in healthy control cells as well as in PC keratinocytes after induction of differentiation by calcium addition (Fig. 5a–c). Accordingly, optineurin and p62/SQSTM1 were unaffected at the protein level (Fig. 5d–e). Therefore, differential expression of key players in autophagosome formation and maturation are most likely not the cause of disturbed mitophagy in PC keratinocytes.

Autolysosome maturation is perturbed in pachyonychia congenita keratinocytes

We next asked whether autolysosome formation is affected in PC keratinocytes. The process of autolysosome formation can be monitored by using an LC3 red fluorescent protein (RFP)–GFP tandem fluorophore. LC3 specifically localizes to

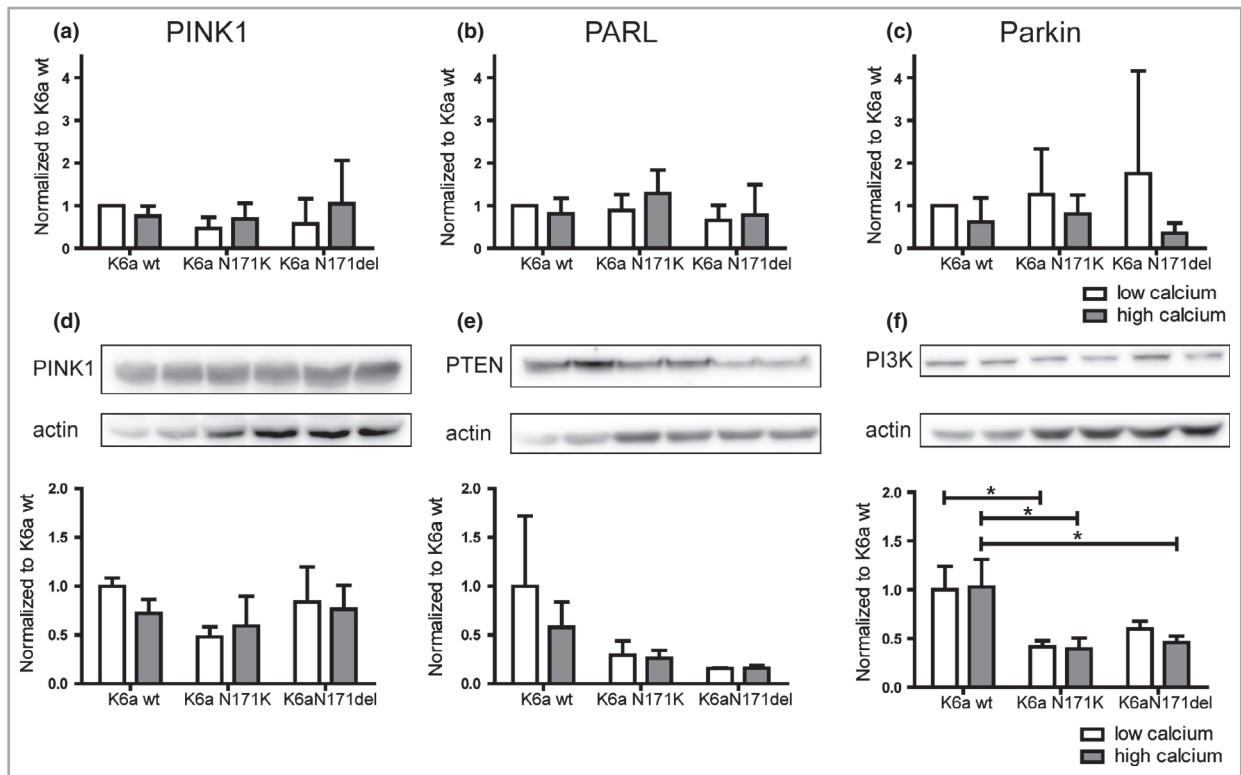
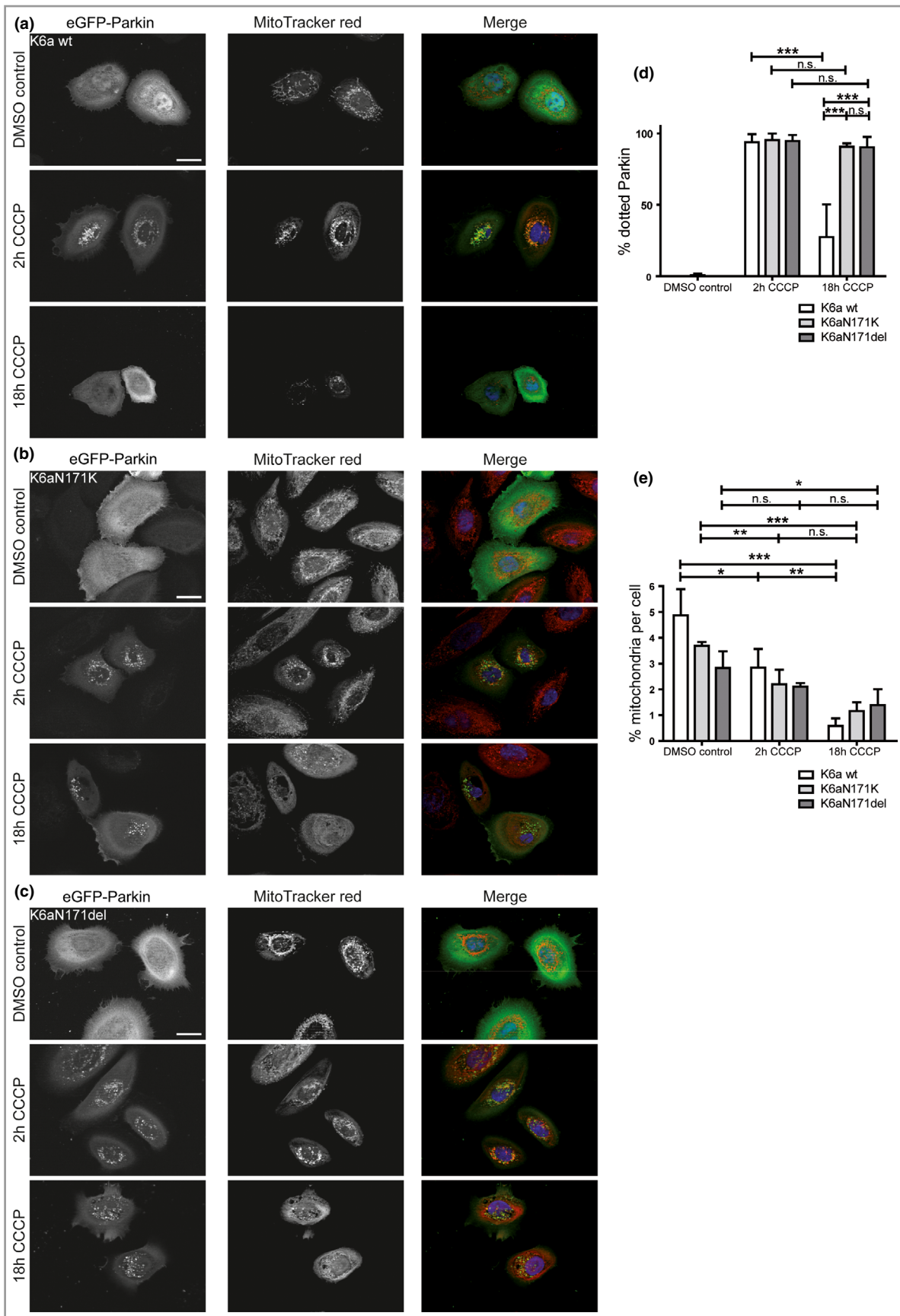


Fig 3. Expression levels of early mitophagy markers are not affected by keratin 6a (K6a) mutations. (a–c) Histogram depicting the results of quantitative polymerase chain reaction (mean \pm SD of three independent experiments each) determining mRNA levels of the early mitophagy markers PINK1 (a); PINK1-cleaving protease PARL (b); and Parkin (c), in K6a wt and mutant K6aN171K and K6aN171del keratinocytes, which were grown under low- and high-calcium conditions. No significant alterations are detectable. (d–f) Results of immunoblot analysis of lysates prepared from the same cell lines (top: examples of immunoblot images; bottom: histograms depicting results of three independent experiments; mean \pm SD) reveal that PINK1 protein levels are also not significantly altered (d) but that its inducer PTEN is slightly decreased (e) and that the PTEN antagonist PI3K is significantly decreased in K6aN171K cells under low- and high-calcium conditions and in K6aN171del keratinocytes under high-calcium conditions, compared with K6a wt. Comparisons between groups were performed using one-way ANOVA with Bonferroni post-hoc test. * $P < 0.05$.

autophagic membranes of autophagosomes and autolysosomes.²⁷ The fusion protein fluoresces both green and red under steady-state conditions. After induction of mitophagy, mRFP-GFP-LC3-containing autophagosomes fuse with lysosomes to form autolysosomes and lose their green fluorescence due to lysosomal acidic and degradative conditions.²¹ The total number of autolysosomes per cell was already elevated under steady-state low-calcium conditions in K6aN171K

and K6aN171del keratinocytes compared with healthy control keratinocytes (61.99 autolysosomes per cell in control cells, 105.6 autolysosomes per cell in K6aN171K PC cells, and 80.88 autolysosomes per cell in K6aN171del PC cells) (Fig. 6a–c upper panels; quantification in Fig. 6e). While calcium addition did not alter the number of autolysosomes in control cells, the number of autolysosomes per cell was significantly increased in both PC cell lines (69.7 autolysosomes per

Fig 4. Mitophagy is severely impaired in pachyonychia congenita keratinocytes. Keratinocytes were transfected with a green fluorescent protein (GFP)–Parkin reporter (eGFP-Parkin) 1 day after seeding, and treated with the mitophagy inducer carbonyl cyanide *m*-chlorophenyl hydrazone (CCCP) 10 $\mu\text{mol L}^{-1}$ for 2 h and 18 h or with dimethyl sulfoxide (DMSO) as a control for 18 h, stained with MitoTracker and subsequently fixed. (a–c) Representative fluorescence micrographs of three independent experiments with at least 48 cells per condition each. Scale bars = 20 μm . (d) Histogram of the percentage (mean \pm SD) of cells displaying either dotted or diffuse cytoplasmic Parkin. All cell lines display an even cytoplasmic Parkin distribution under control conditions (a–d) shifting to dotted, i.e. mitochondrial-targeted Parkin, after 2 h of CCCP treatment as expected for dysfunctional mitochondria. However, after 18 h of CCCP treatment, only 73% of keratin 6a (K6a) wild-type (wt) keratinocytes display a restored cytoplasmic Parkin distribution (a, e), whereas 91% of K6aN171K and 90% of K6aN171del cells still display dotted Parkin (b, c, e). (e) Histogram depicting percentage (mean \pm SD) of cell area covered by mitochondria. Note that mitochondrial area is significantly reduced in K6a wt cells by CCCP (5% in untreated cells, 3% after 2 h of CCCP, 0.6% after 18 h of CCCP); however, mitochondrial area in PC cell lines only changes within 2 h of CCCP treatment but not further after 18 h of CCCP treatment. Comparisons between groups were performed using one-way ANOVA with Bonferroni post-hoc test. * $P < 0.05$, ** $P < 0.01$, *** $P < 0.001$; n.s., not significant.



cell in control cells, 138.0 autolysosomes per cell in K6aN171K PC cells, and 152.5 autolysosomes per cell in K6aN171del PC cells) (Fig. 6a–c lower panels; quantification in Fig. 6e). Likewise, while the percentage of autolysosomes (only red LC3 puncta) was not altered in low-calcium conditions compared with wt control cells, elevation of extracellular calcium led to a significantly increased percentage of autolysosomes in PC cells (58% vs. 57% in control cells, 55% vs. 71% in K6aN171K PC cells, and 64% vs. 83% in K6aN171del PC cells) (Fig. 6d).

Taken together, these results indicate that autolysosome generation is unaffected but that autolysosomal recycling is severely impaired in cells derived from patients with PC.

Discussion

In this paper, we addressed the possible role of mitophagy in the pathogenesis of PC. To this end we used two patient-derived keratinocyte cell lines with different mutations in K6a: K6aN171K and K6aN171del. We showed that in PC, old mitochondria accumulate over a time period of 48 h and that CCCP-induced mitochondrial clearance is delayed. Still, early

and late mitophagy markers are not changed. While autolysosome formation is not affected, autolysosomes accumulate because of compromised maturation or recycling, suggesting a role of K6a in autolysosomal turnover.

Autophagy is a conserved process that leads to the lysosomal degradation of cellular components such as proteins and organelles. Elimination of old or dysfunctional mitochondria via autophagy is called mitophagy. Disturbed mitophagy and autophagy lead to a number of human diseases such as cardiomyopathies, and neurodegenerative and skin diseases.^{28,29} Functional autophagy is especially important in terminal differentiation of keratinocytes, which lose their organelles during the course of keratinization to become dead corneocytes in the outermost epidermal layer. Accumulation of autolysosomes could only be seen after calcium-induced differentiation of PC keratinocytes. There have been several reports that confirm the role of autophagy in keratinocyte differentiation. For example, mice lacking Atg7, which is important for autophagosome assembly, have a low level of autophagy and show epidermal acanthosis and hyperkeratosis.¹⁶ Keratinocytes treated with the autophagy inhibitors 3-methyladenine or wortmannin present enhanced inflammatory responses and

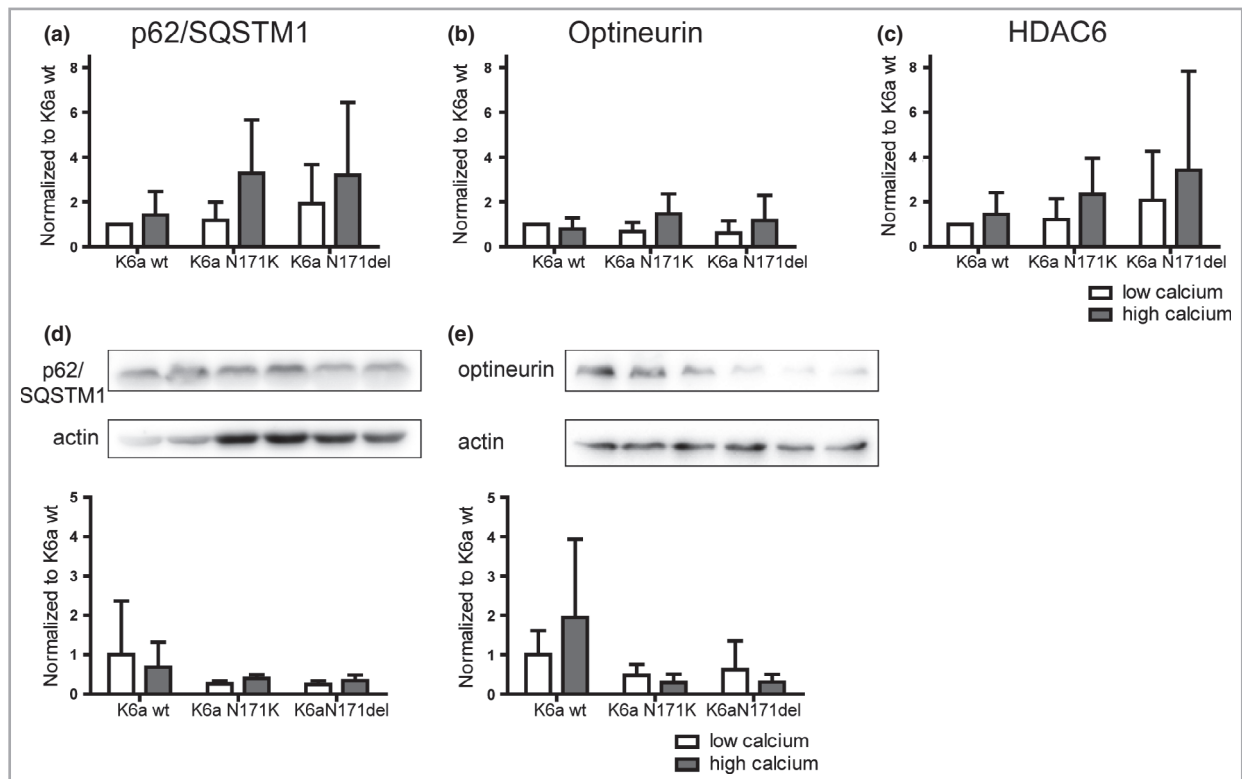


Fig 5. Expression levels of markers for autophagosome formation are not affected by keratin 6a (K6a) mutations. (a–c) Histograms of autophagosomal mRNA levels (mean ± SD) were prepared from quantitative polymerase chain reaction analyses of three independent experiments from cells grown at low- and high-calcium conditions. Neither p62/SQSTM1 (a) nor optineurin (b) nor HDAC6 (c) show significant alterations of mRNA levels in mutant K6aN171K and K6aN171del compared with K6a wt keratinocytes. (d, e) Immunoblot analyses of cell lysates from the same cell lines further demonstrate that p62/SQSTM1 (d) and optineurin (e) protein levels are also not altered in the mutant cell lines. Corresponding histograms of protein levels (mean ± SD of three independent experiments) are shown below. Comparisons between groups were performed using one-way ANOVA with Bonferroni post-hoc test.

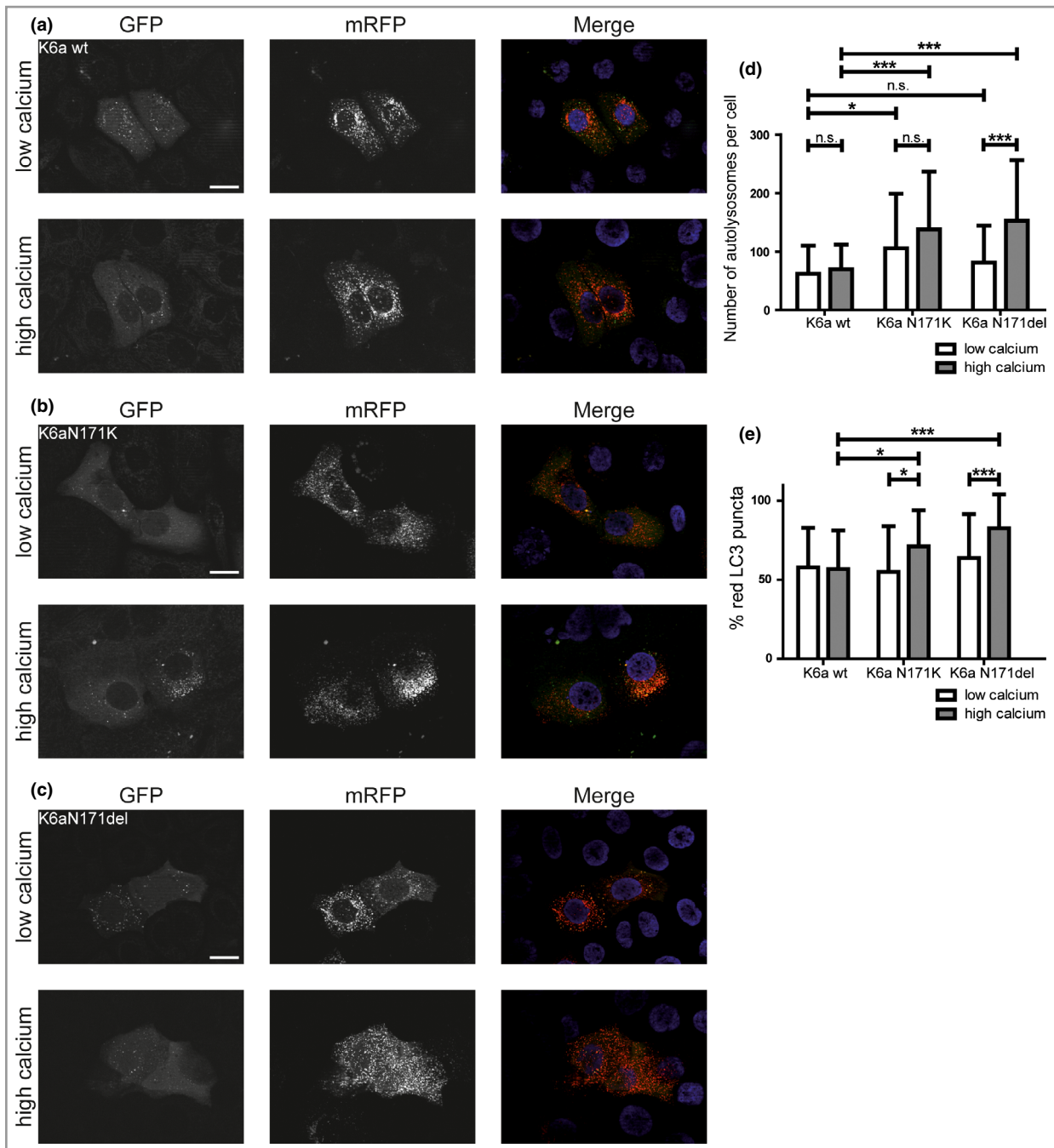


Fig 6. Keratin 6a (K6a) mutations lead to impaired autolysosome maturation and recycling. To monitor autophagosome and autolysosome formation, cells were transfected with an LC3 red fluorescent protein (RFP)–green fluorescent protein (GFP) tandem fluorophore. Autophagosomes are represented by green and red puncta, whereas autolysosomes show only red fluorescence. (a–c) The representative fluorescence micrographs (three independent experiments of $n \geq 16$ cells per condition each) taken from keratinocytes grown at low- and high-calcium conditions show that the total number of red-only puncta (autolysosomes) is significantly increased in pachyonychia congenita cell lines compared with K6a wild-type (wt) cells grown at high calcium [histogram in (d)]. Furthermore, the percentage of red-only puncta is significantly increased at high-calcium compared with low-calcium conditions in both of the mutant cell lines but not in K6a wt keratinocytes [quantification in (e)]. Scale bars = 20 μm . Comparisons between groups were performed using one-way ANOVA with Bonferroni post-hoc test. * $P < 0.05$, *** $P < 0.001$; n.s., not significant.

increased cell proliferation.³⁰ Furthermore, autophagy-deficient keratinocytes display a weakened stress response resulting in DNA damage, cell cycle arrest and premature ageing.³¹

Autophagy is vital for cells to survive stresses as it eliminates damaged proteins and organelles, and thus restores cell health. Part of the stress response in keratinocytes after wounding is the

upregulation of keratins 6, 16 and 17.³² Keratin 6 has been linked to cell migration and wound healing.^{4,33} While to date not much is known about the influence of autophagy on wound healing, it was shown that ATG7 knockdown stimulated cell migration while inhibition of MTORC1 by rapamycin enhanced autophagy and reduced cell migration.³⁴

A role of intermediate filaments in mitochondrial homeostasis has been pointed out in several reports (reviewed in Schwarz and Leube⁵), but no clear functional connection has yet been established. For example, it has been shown that desmin mutations lead to a disturbed mitochondria–ER distance.³⁵ Mitochondria–ER contact sites are important for the formation of the omegasome, a membranous structure that engulfs damaged mitochondria in order to form autophagosomes.³⁶ Although mitochondria–ER contact sites were reduced in PC cells, autophagosome formation seemed to be unaffected. Additionally, MAMs are specialized domains for intracellular calcium transfer, shuttling calcium from ER to the mitochondrial matrix.³⁷ Intracellular calcium acts as a regulator of autophagy by inhibiting MTORC1, and therefore activates autophagy. Loss of mitochondria–ER contact sites, as well as a decrease in mitochondrial calcium and an increase in cytoplasmic calcium, leads to autophagy.^{38,39} Elevation of intracellular calcium of keratinocytes additionally induces their differentiation, explaining why the effects of PC mutations on autophagy can be seen after calcium treatment.⁴⁰ K6a mutations may act on two different levels, (i) by disturbing mitochondria–ER calcium handling, which results in enhanced autophagy, and (ii) by disturbing autolysosomal recycling.

Autolysosomal reformation is the process in which lysosomal components of autolysosomes are recycled in order to reform lysosomes. During this reformation, tubules protrude from the autolysosomal membrane and form protolysosomes, which initially lack lysosomal acidity. Those tubules then become acidic and mature into lysosomes. Rab7, a vesicle transport regulator, and KIF5B, a member of the kinesin 1 family, are two important factors for autolysosomal recycling.^{12,41} KIF5B has been implicated in the control of intermediate filament localization in heart muscle, while Rab7 has been shown to directly interact with the intermediate filament vimentin.^{13,42} Additionally, vimentin, as well as keratin intermediate filaments, have been shown to move along microtubules with the help of KIF5B.⁴³ Furthermore, it has recently been shown that autophagy and lysosomal functions play an important role in keratinocyte differentiation in organotypic human skin where lysosomes promote mitochondrial metabolism and the associated production of mitochondrial ROS, which in turn triggers autophagy on its release into the cytoplasm of suprabasal keratinocytes.⁴⁴

Autolysosomal reformation is upregulated during stress situations; it depends on mTOR signalling and can be blocked by the mTOR inhibitor rapamycin.^{15,45} In contrast, rapamycin treatment also induces autophagy, providing a feedback mechanism to avoid excessive cell-harming autophagy.⁴⁵ Furthermore, rapamycin blocks K6a expression in human keratinocytes and ameliorates PC symptoms.⁴⁶

Here, we show for the first time that mitophagy and autolysosomal turnover are disturbed in the keratinocytes of patients with PC. Further investigations clarifying the interplay between autophagy and epidermal differentiation are necessary to understand PC pathogenesis.

Acknowledgments

We are especially grateful to the pachyonychia congenita community and Leonard M. Milstone, for kindly providing the used cell lines. We thank the EB house Austria for the wild-type cell line. We thank Sven Geisler, Tamotsu Yoshimori and Zhen Yan for plasmids.

References

- Omary MB. “IF-pathies”: a broad spectrum of intermediate filament-associated diseases. *J Clin Invest* 2009; **119**:1756–62.
- McLean WHI, Rugg EL, Lunny DP *et al.* Keratin 16 and keratin 17 mutations cause pachyonychia congenita. *Nat Genet* 1995; **9**:273–8.
- Leachman SA, Kaspar RL, Fleckman P *et al.* Clinical and pathological features of pachyonychia congenita. *J Invest Dermatol Symp Proc* 2005; **10**:3–17.
- Wong P, Coulombe PA. Loss of keratin 6 (K6) proteins reveals a function for intermediate filaments during wound repair. *J Cell Biol* 2003; **163**:327–37.
- Schwarz N, Leube RE. Intermediate filaments as organizers of cellular space: how they affect mitochondrial structure and function. *Cells* 2016; **5**:30.
- Ni H-M, Williams JA, Ding W-X. Mitochondrial dynamics and mitochondrial quality control. *Redox Biol* 2015; **4**:6–13.
- Meissner C, Lorenz H, Weihofen A *et al.* The mitochondrial intramembrane protease PARL cleaves human Pink1 to regulate Pink1 trafficking. *J Neurochem* 2011; **117**:856–67.
- Jin SM, Lazarou M, Wang C *et al.* Mitochondrial membrane potential regulates PINK1 import and proteolytic destabilization by PARL. *J Cell Biol* 2010; **191**:933–42.
- Pankiv S, Clausen TH, Lamark T *et al.* p62/SQSTM1 binds directly to Atg8/LC3 to facilitate degradation of ubiquitinated protein aggregates by autophagy. *J Biol Chem* 2007; **282**:24131–45.
- Narendra DP, Kane LA, Hauser DN *et al.* p62/SQSTM1 is required for Parkin-induced mitochondrial clustering but not mitophagy; VDAC1 is dispensable for both. *Autophagy* 2010; **6**:1090–106.
- Wong YC, Holzbaur ELF. Optineurin is an autophagy receptor for damaged mitochondria in parkin-mediated mitophagy that is disrupted by an ALS-linked mutation. *Proc Natl Acad Sci U S A* 2014; **111**:E4439–48.
- Kuchitsu Y, Homma Y, Fujita N, Fukuda M. Rab7 knockout unveils regulated autolysosome maturation induced by glutamine starvation. *J Cell Sci* 2018; **131**:jcs215442.
- Cogli L, Progidia C, Bramato R, Bucci C. Vimentin phosphorylation and assembly are regulated by the small GTPase Rab7a. *Biochim Biophys Acta* 2013; **1833**:1283–93.
- Blankson H, Holen I, Seglen PO. Disruption of the cytokeratin cytoskeleton and inhibition of hepatocytic autophagy by okadaic acid. *Exp Cell Res* 1995; **218**:522–30.
- Yu L, McPhee CK, Zheng L *et al.* Autophagy termination and lysosome reformation regulated by mTOR. *Nature* 2010; **465**:942–6.
- Yoshihara N, Ueno T, Takagi A *et al.* The significant role of autophagy in the granular layer in normal skin differentiation and hair growth. *Arch Dermatol Res* 2015; **307**:159–69.

- 17 Akinduro O, Sully K, Patel A *et al.* Constitutive autophagy and nucleophagy during epidermal differentiation. *J Invest Dermatol* 2016; **136**:1460–70.
- 18 Halbert CL, Demers GW, Galloway DA. The E6 and E7 genes of human papillomavirus type 6 have weak immortalizing activity in human epithelial cells. *J Virol* 1992; **66**:2125–34.
- 19 Schindelin J, Arganda-Carreras I, Frise E *et al.* Fiji – an Open Source platform for biological image analysis. *Nat Methods* 2012; **9**:676–82.
- 20 Rueden CT, Schindelin J, Hiner MC *et al.* Image J2: ImageJ for the next generation of scientific image data. *BMC Bioinformatics* 2017; **18**:529.
- 21 Kimura S, Noda T, Yoshimori T. Dissection of the autophagosome maturation process by a novel reporter protein, tandem fluorescent-tagged LC3. *Autophagy* 2007; **3**:452–60.
- 22 Hernandez G, Thornton C, Stotland A *et al.* MitoTimer: a novel tool for monitoring mitochondrial turnover. *Autophagy* 2013; **9**:1852–61.
- 23 Gelmetti V, De Rosa P, Torosantucci L *et al.* PINK1 and BECN1 relocate at mitochondria-associated membranes during mitophagy and promote ER-mitochondria tethering and autophagosome formation. *Autophagy* 2017; **13**:654–69.
- 24 Okatsu K, Oka T, Iguchi M *et al.* PINK1 autophosphorylation upon membrane potential dissipation is essential for Parkin recruitment to damaged mitochondria. *Nat Commun* 2012; **3**:1016.
- 25 Iwata A, Riley BE, Johnston JA, Kopito RR. HDAC6 and microtubules are required for autophagic degradation of aggregated huntingtin. *J Biol Chem* 2005; **280**:40282–92.
- 26 Lee J-Y, Koga H, Kawaguchi Y, *et al.* HDAC6 controls autophagosome maturation essential for ubiquitin-selective quality-control autophagy. *EMBO J* 2010; **29**:969–80.
- 27 Kabeya Y, Mizushima N, Ueno T *et al.* LC3, a mammalian homologue of yeast Apg8p, is localized in autophagosomal membranes after processing. *EMBO J* 2000; **19**:5720–8.
- 28 Yu T, Zuber J, Li J. Targeting autophagy in skin diseases. *J Mol Med (Berl)* 2015; **93**:31–8.
- 29 Um J-H, Yun J. Emerging role of mitophagy in human diseases and physiology. *BMB Rep* 2017; **50**:299–307.
- 30 Lee H-M, Shin D-M, Yuk J-M *et al.* Autophagy Negatively Regulates Keratinocyte Inflammatory Responses via Scaffolding Protein p62/SQSTM1. *J Immunol* 2011; **186**:1248–58.
- 31 Song X, Narzt MS, Nagelreiter IM *et al.* Autophagy deficient keratinocytes display increased DNA damage, senescence and aberrant lipid composition after oxidative stress in vitro and in vivo. *Redox Biol* 2017; **11**:219–30.
- 32 Onset of re-epithelialization after skin injury correlates with a reorganization of keratin filaments in wound edge keratinocytes: defining a potential role for keratin 16. *J Cell Biol* 1996; **132**:381–97.
- 33 Wojcik SM, Bundman DS, Roop DR. Delayed wound healing in keratin 6a knockout mice. *Mol Cell Biol* 2000; **20**:5248–55.
- 34 Tuloup-Minguez V, Hamai A, Greffard A *et al.* Autophagy modulates cell migration and β 1 integrin membrane recycling. *Cell Cycle* 2013; **12**:3317–28.
- 35 Diokmetzidou A, Soumaka E, Kloukina I *et al.* Desmin and α B-crystallin interplay in the maintenance of mitochondrial homeostasis and cardiomyocyte survival. *J Cell Sci* 2016; **129**:3705–20.
- 36 Axe EL, Walker SA, Manifava M *et al.* Autophagosome formation from membrane compartments enriched in phosphatidylinositol 3-phosphate and dynamically connected to the endoplasmic reticulum. *J Cell Biol* 2008; **182**:685–701.
- 37 Rizzuto R, Pinton P, Carrington W *et al.* Close contacts with the endoplasmic reticulum as determinants of mitochondrial Ca^{2+} responses. *Science* 1998; **280**:1763–6.
- 38 Cárdenas C, Foskett JK. Mitochondrial Ca^{2+} signals in autophagy. *Cell Calcium* 2012; **52**:44–51.
- 39 Gomez-Suaga P, Paillusson S, Stoica R *et al.* The ER-mitochondria tethering complex VAPB-PTPIP51 regulates autophagy. *Curr Biol* 2017; **27**:371–85.
- 40 Hennings H, Michael D, Cheng C *et al.* Calcium regulation of growth and differentiation of mouse epidermal cells in culture. *Cell* 1980; **19**:245–54.
- 41 Du W, Su QP, Chen Y *et al.* Kinesin 1 drives autolysosomal tubulation. *Dev Cell* 2016; **37**:326–36.
- 42 Wang Z, Cui J, Wong WM *et al.* Kif5b controls the localization of myofibril components for their assembly and linkage to the myotendinous junctions. *Development* 2013; **140**:617–26.
- 43 Robert A, Tian P, Adam SA *et al.* Kinesin-dependent transport of keratin filaments: a unified mechanism for intermediate filament transport. *FASEB J* 2018; **33**:388–99.
- 44 Monteleon CL, Agnihotri T, Dahal A *et al.* Lysosomes support the degradation, signaling, and mitochondrial metabolism necessary for human epidermal differentiation. *J Invest Dermatol* 2018; **138**:1945–54.
- 45 Zhang J, Zhou W, Lin J *et al.* Autophagic lysosomal reformation depends on mTOR reactivation in H₂O₂-induced autophagy. *Int J Biochem Cell Biol* 2016; **70**:76–81.
- 46 Hickerson RP, Leake D, Pho LN *et al.* Rapamycin selectively inhibits expression of an inducible keratin (K6a) in human keratinocytes and improves symptoms in pachyonychia congenita patients. *J Dermatol Sci* 2009; **56**:82–8.